Supporting Information

The controlled synthesis of PdAg alloy nanospheres and the selective oxidation for ethylene glycol

Anqi Zhao[a], Mengyun Hu[a], Jie Li[a], Xinyu Gu[a], Changqing Ye[b,] *, Yukou Du[a,] *

[a] *College of Chemistry, Chemical Engineering and Materials Science, Soochow University, 199 Renai Road, Suzhou 215123, P.R. China*

[b] *Jiangsu Key Laboratory for Environment Functional Materials, School of Materials Science and Engineering, Suzhou University of Science and Technology, Suzhou 215009, P.R. China*

E-mail addresses: yechangqing@mail.usts.edu.cn (C. Ye); duyk@suda.edu.cn (Y. Du)

Experimental section

Materials characterization

TEM was performed on HT7700 at 120 kV, and High-resolution Transmission electron microscope (HRTEM) was tested on Talos F200X G2 at 200 kV to characterize the structures of the samples. The phase structure was analyzed by X-ray diffraction (XRD) spectra. The scanning electron microscope energy dispersive X-ray spectroscopy (SEM-EDS) was collected on EVO18 at 15 kV, and X-ray photoelectron spectroscopy (XPS) techniques were conducted to analyze the element composition and chemical states of catalysts.

Electrochemical Measurements

The CHI660 electrochemistry workstation was utilized to accomplish all the electrochemical tests with a three-electrode cell system, including a saturated calomel (SCE) served as the reference electrode, a platinum electrode worked as contrast electrode, glass carbon electrode (GCE) with a diameter of 5 mm acted as working electrode and 1 M KOH + 1 M alcohol solution was used to construct electrolyte for further measurements. The catalysts were loaded on carbon powder (20 wt.%) and then mixed with isopropanol to make an ink solution (0.2 mg mL^{-1}) that was used to investigate electrocatalytic activity for EGOR with 20 wt% commercial Pd/C serving as benchmarks.

Cyclic voltammetry (CV) was conducted in 1 M KOH + 1 M EG solution, where the potentials were set at -0.8 ~ 0.4 V vs. SCE, the sweep speed was set to 50 mV s^{-1}, and the final potentials were converted according to the equation:

$$E_{RHE} = E + 0.059 \times pH + 1.067$$

Chronoamperometry (CA) was conducted to test the stability of catalysts for 4000 s.

Product analysis

4 mg of catalyst was dispersed in 2 mL of isopropanol, and 10 μL of 5 wt.% Nafion

was added as a binder. After 30 minutes of ultrasonication, the uniformly dispersed catalyst ink was loaded on 1 ×1 cm^2 carbon paper, dried with an infrared lamp, and placed on the clip electrode for further use. The CA test was conducted to obtain electrolytes in 1 M EG + 1 M KOH solution at a constant amount of charge (77 C). The products were quantified by external standard calibration curves (**Fig. S10**) via HPLC (Shimadzu corporation, LC-2050) equipped with organic acid column (Bio-Rad, Aminex HPX-87H) using 5 mM aqueous H_2SO_4 as mobile phase (0.6 mL min^{-1}, 65°C) and detected by UV detector (210 nm).

The Faraday efficiency (FE, %) of the product formation can be determined by the following equation:

$$\text{FE (\%)} = \frac{n_e \times n_{product} \times F}{Q}$$

Where n_e is the number of electrons required to oxidize products in per reaction. $n_{product}$ (mol) is the productivity of products, F is the Faraday constant (F = 96485 C·mol^{-1}), and Q is the total charge passed through the electrode.

Supplementary figures

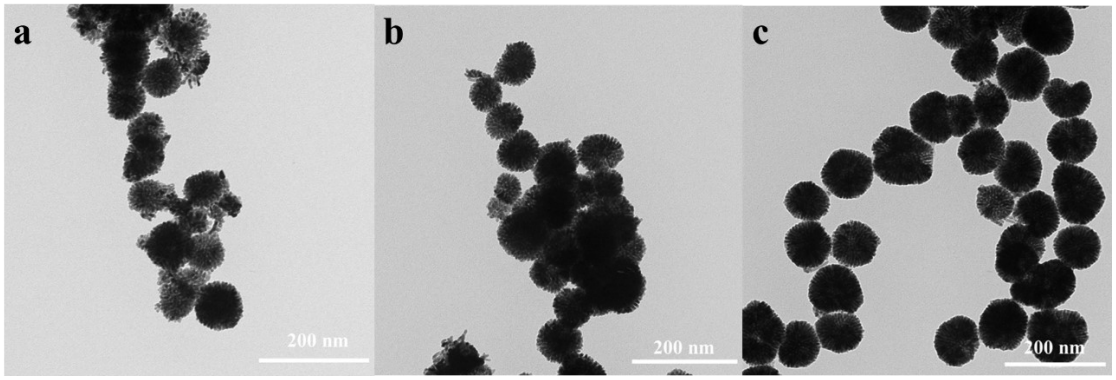

Fig. S1. TEM images of (a) PdAg NSs, (b) Pd_2Ag NSs, and (c) Pd_4Ag NSs.

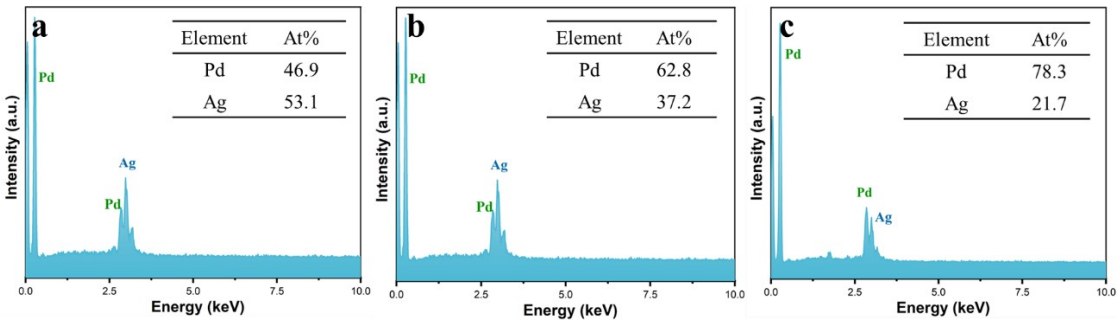

Fig. S2. SEM-EDS of (a) PdAg NSs, (b) Pd_2Ag NSs, and (c) Pd_4Ag NSs.

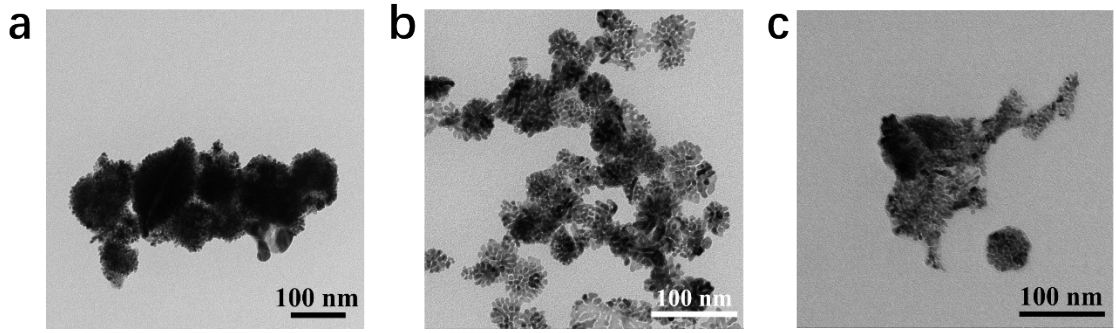

Fig. S3. (a) TEM image of Pd_4Ag NSs prepared at 25 °C. (b) TEM image of Pd_4Ag NSs prepared in a mixed solvent of 2 mL ethanol and 8 mL water. (c) TEM image of pure Pd.

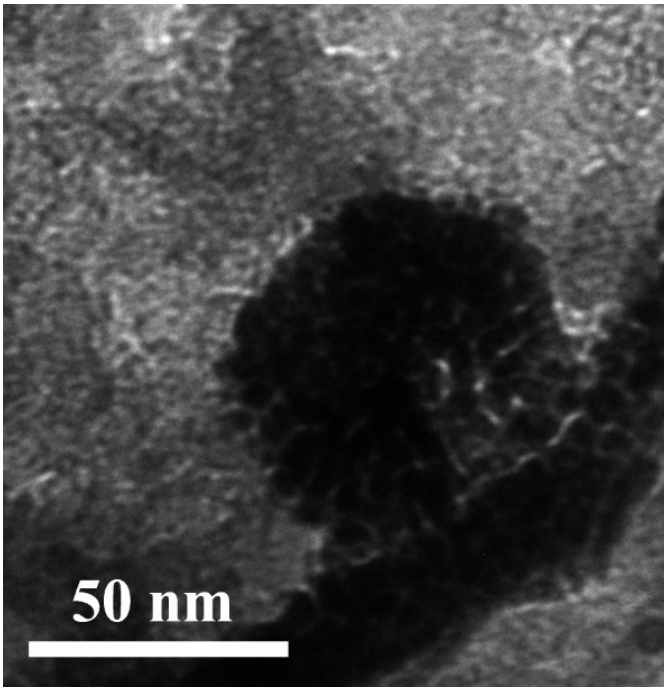

Fig. S4. TEM images of Pd_4Ag NSs after CVs.

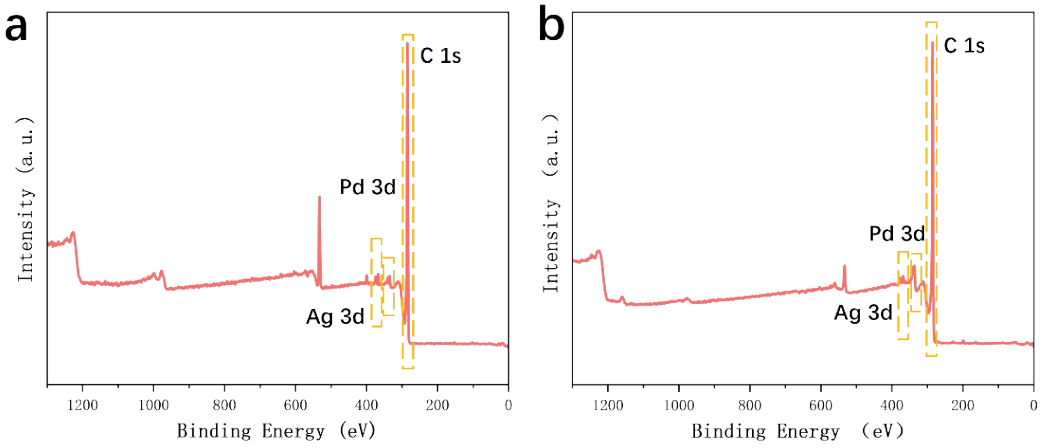

Fig. S5. Survey XPS spectra of Pd_4Ag NSs (a) before and (b) after CV tests.

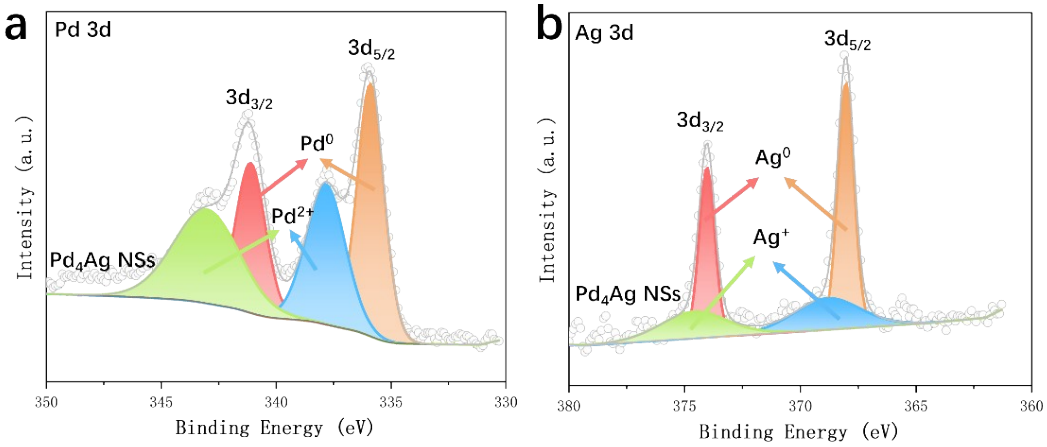

Fig. S6. (a) Pd 3d and (b) Ag 3d XPS spectra of Pd_4Ag NSs after CV tests.

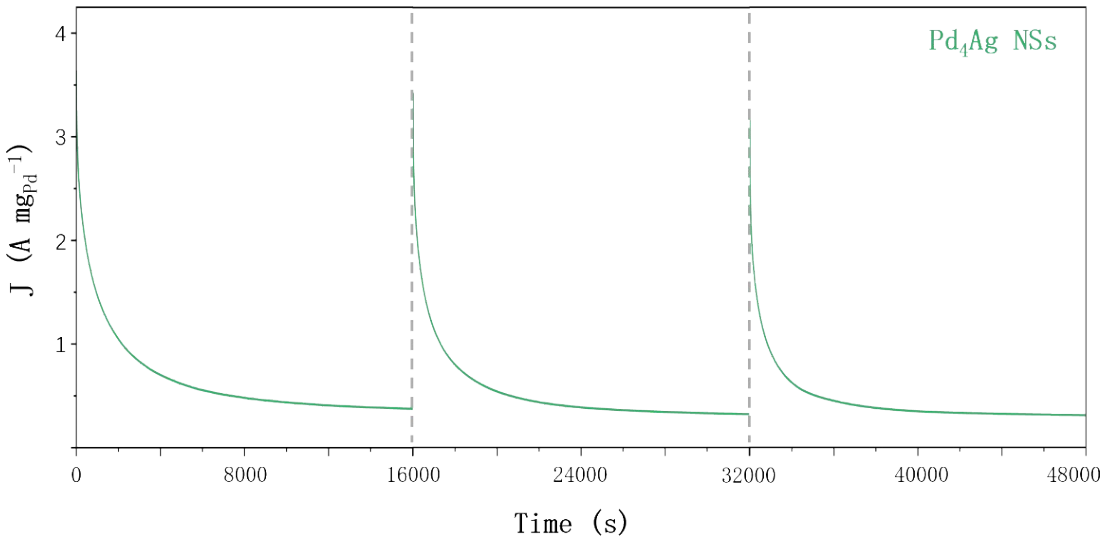

Fig. S7. The i-t curve of Pd_4Ag NSs for EGOR at 0.94 V (vs. RHE).

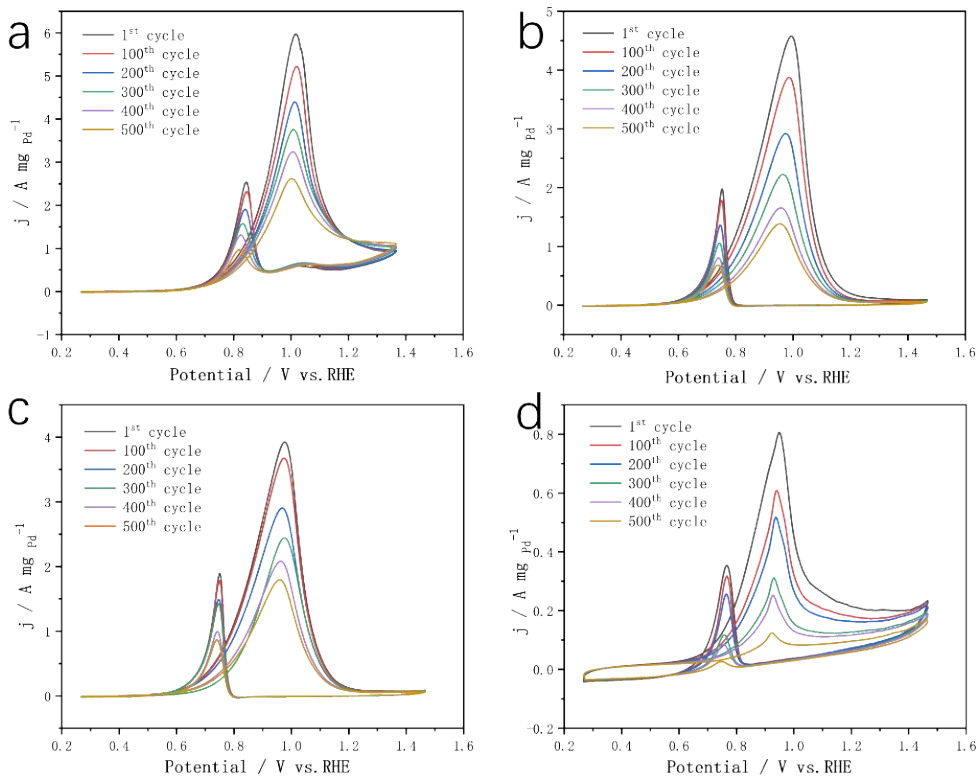

Fig. S8. CV curves of 500 cycles of (a) Pd_4Ag NSs, (b) Pd_2Ag NSs, (c) PdAg NSs, and (d) Pd/C in 1 mol L^{-1} KOH + 1 mol L^{-1} ethylene glycol solution.

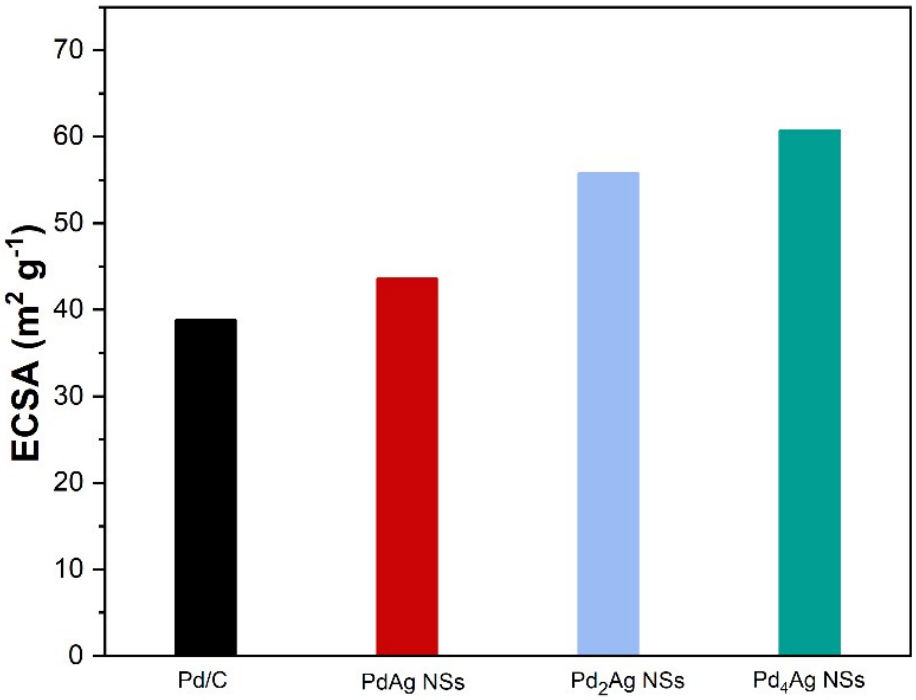

Fig. S9. Electrochemical active surface areas of Pd/C, PdAg NSs, Pd_2Ag NSs, Pd_4Ag NSs

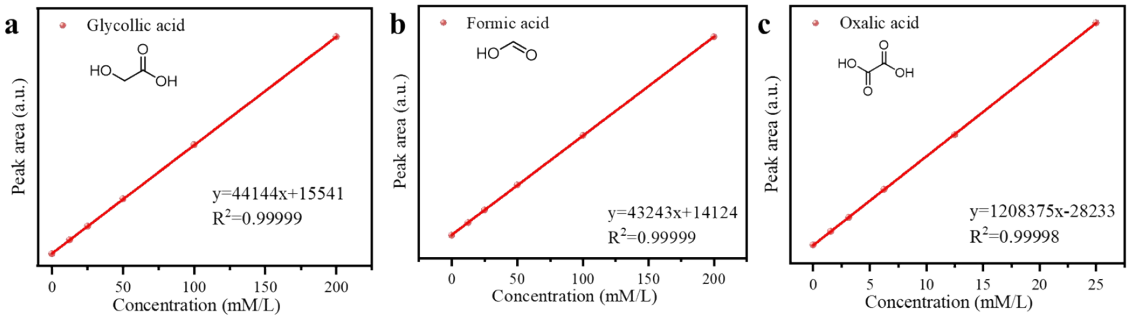

Fig. S10. (a-c) The calibration curves of glycolic acid, formic acid, and oxalic acid according to the HPLC, respectively.

Table S1. Summary of Faradaic Efficiency (FE) of various products for ethylene glycol electrooxidation reaction over Pd_4Ag NSs at different potentials.

Potential / V vs. RHE	FE of oxalic acid	FE of glycolic acid	FE of cleavage products
0.86 V	46%	53%	1%
0.91 V	47%	41%	12%
0.96 V	46%	39%	15%
1.01 V	17%	74%	9%
1.06 V	18%	72%	10%

Table S2. Comparison of EGOR performances of Pd_4Ag NSs and various Pd-based catalysts from published works.

Catalysts	Mass activity	Electrolyte	References
Pd_4Ag NSs	**5.98 A mg_{Pd}^{-1}**	**1 M KOH + 1 M EG**	**This work**
Pd_6Bi TNWs	3.05 A mg_{Pd}^{-1}	1 M KOH + 1 M EG	1
Pd/PANI-rGO	4.34 A mg_{Pd}^{-1}	1 M KOH + 1 M EG	2
Pd_3Pb NDs	2.96 A mg_{Pd}^{-1}	1 M KOH + 1 M EG	3
Ir-CuPd SMTs	7.93 A mg_{Pd}^{-1}	1 M KOH + 1 M EG	4
P-PdMo	4.98 A mg_{Pd}^{-1}	1 M KOH + 1 M EG	5
PdNiRu NSs	3.86 A mg_{Pd}^{-1}	1 M KOH + 1 M EG	6
fcc-2H-fcc Au@Pd	5.4 A mg_{Pd}^{-1}	0.5 M KOH + 0.5 M EG	7

References

1 X. Lao, Z. Li, L. Yang, B. Zhang, W. Ye, A. Fu, P. Guo, Monodispersed ultrathin twisty PdBi alloys nanowires assemblies with tensile strain enhance C2+ alcohols electrooxidation, *J. Energy Chem.*, 2023, ***79***, 279-290.

2 H. Zhang, J. Li, X. Huang, X. Duan, R. Yue, J. Xu, Lamellar polyaniline-modified reduced graphene oxide loaded electron-rich Pd nanoparticles for highly efficient electrooxidation of C2 alcohols, *Fuel*, 2024, ***369***, 131781.

3 T. Sun, J. Chen, X. Lao, X. Zhang, A. Fu, W. Wang, P. Guo, Unveiling the Synergistic Effects of Monodisperse Sea Urchin-like PdPb Alloy Nanodendrites as Stable Electrocatalysts for Ethylene Glycol and Glycerol Oxidation Reactions, *Inorg. Chem.*, 2022, ***61***, 10220-10227.

4 H. Lv, Y. Mao, H. Yao, H. Ma, C. Han, Y. Y. Yang, Z. A. Qiao, B. Liu, Ir-Doped CuPd Single-Crystalline Mesoporous Nanotetrahedrons for Ethylene Glycol Oxidation Electrocatalysis: Enhanced Selective Cleavage of C-C Bond, *Angew. Chem., Int. Ed.*, 2024, ***63***, e202400281.

5 J. Liu, H. Liu, Q. Wang, T. Li, T. Yang, W. Zhang, H. Xu, H. Li, X. Qi, Y. Wang, A. Cabot, Phosphorus doped PdMo bimetallene as a superior bifunctional fuel cell electrocatalyst, *Chem. Eng. J.*, 2024, ***486***, 150258.

6 X. Li, T. Lu, H. Pang, M. Zhang, D. Xu, L. Xu, M. Han, J. Yang, Ultrathin curved PdNiRu nanosheets as bifunctional catalysts for oxygen reduction and ethylene glycol oxidation, *Nano Research*, 2023, ***17***, 3777-3784.

7 X. Zhou, Y. Ma, Y. Ge, S. Zhu, Y. Cui, B. Chen, L. Liao, Q. Yun, Z. He, H. Long; et al., Preparation of Au@Pd Core–Shell Nanorods with fcc-2H-fcc Heterophase for Highly Efficient Electrocatalytic Alcohol Oxidation, *J. Am. Chem. Soc.*, 2021, ***144***, 547-555.